AD-A073 008 MINNESOTA UNIV MINNEAPOLIS DEPT OF AEROSPACE ENGINE--ETC F/G 20/11
STRUCTURAL INELASTICITY XXIII. A PIECEWISE LINEAR THEORY OF PLA--ETC(U)
NOV 78 P G HODGE N00014-75-C-0177
UNCLASSIFIED AEM-H1-23 NL

| OF |
AD
A073008

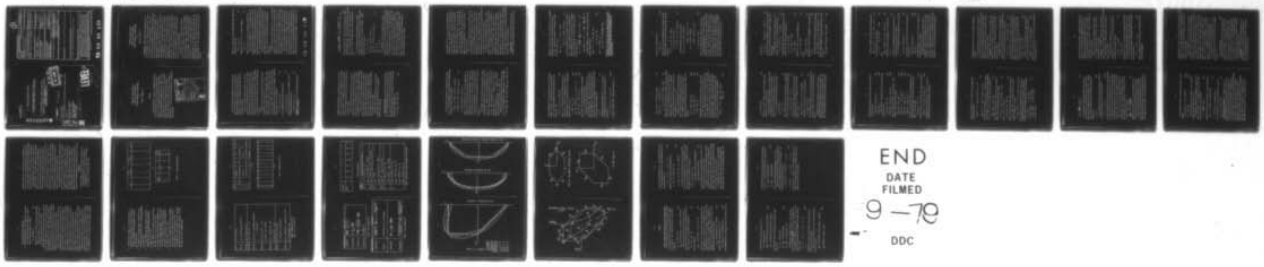

END
DATE
FILMED
9-79
DDC

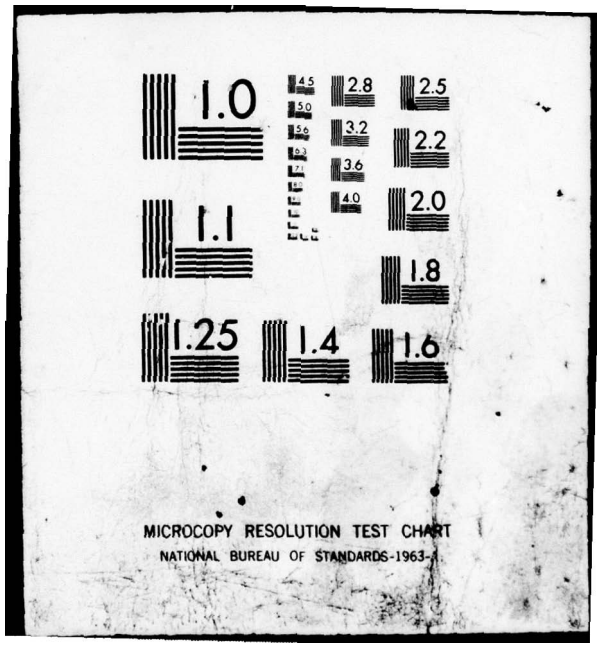
1.0
1.1
1.25
1.4
1.6
1.8
2.0
2.2
2.5
2.8
3.2
3.6
4.0
4.5
5.0
5.6
6.3
MICROCOPY RESOLUTION TEST CHART
NATIONAL BUREAU OF STANDARDS-1963-A

Report AEM-H1-23

(14)

(6) STRUCTURAL INELASTICITY XXIII

A Piecewise Linear Theory of Plasticity for an Initially Isotropic Material in Plane Stress

(10) Philip G. Hodge, Jr., Professor of Mechanics

Department of Aerospace Engineering and Mechanics
University of Minnesota
Minneapolis, Minnesota 55455

(11) November 1978 (12) 22 p.

(9) Technical Report,

Qualified requesters may obtain copies of this report from DDC

Prepared for

OFFICE OF NAVAL RESEARCH
Arlington, VA 22217

OFFICE OF NAVAL RESEARCH
CHicago Branch Office
536 South Clark St.
Chicago, IL 60605

(15) N00014-75-C-0177

LEVEL II

A058276

(1)

SECURITY CLASSIFICATION OF THIS PAGE (When Data Entered)

REPORT DOCUMENTATION PAGE		READ INSTRUCTIONS BEFORE COMPLETING FORM
1. REPORT NUMBER: AEM-H1-23	2. GOVT ACCESSION NO.	3. RECIPIENT'S CATALOG NUMBER
4. TITLE (and Subtitle): STRUCTURAL INELASTICITY XXIII A Piecewise Linear Theory of Plasticity for an Initially Isotropic Material in Plane Stress		5. TYPE OF REPORT & PERIOD COVERED 6. PERFORMING ORG. REPORT NUMBER
7. AUTHOR(s): Philip G. Hodge, Jr. Prof. of Mechanics		8. CONTRACT OR GRANT NUMBER(s): N14-75-C-0177
9. PERFORMING ORGANIZATION NAME AND ADDRESS: University of Minnesota, Minneapolis, Minnesota 55455		10. PROGRAM ELEMENT, PROJECT, TASK AREA & WORK UNIT NUMBERS: NR 064-429
11. CONTROLLING OFFICE NAME AND ADDRESS: OFFICE OF NAVAL RESEARCH, Arlington, VA 22217		12. REPORT DATE: November, 1978 13. NUMBER OF PAGES: 41
14. MONITORING AGENCY NAME & ADDRESS(if different from Controlling Office): OFFICE OF NAVAL RESEARCH, Chicago Branch Office, 536 South Clark St., Chicago, IL 60605		15. SECURITY CLASS. (of this report): Unclassified 15a. DECLASSIFICATION/DOWNGRADING SCHEDULE

16. DISTRIBUTION STATEMENT (of this Report)

Qualified requesters may obtain copies of this report from DDC

This document has been approved for public release and sale; its distribution is unlimited.

17. DISTRIBUTION STATEMENT (of the abstract entered in Block 20, if different from Report)

18. SUPPLEMENTARY NOTES

19. KEY WORDS (Continue on reverse side if necessary and identify by block number)

Plasticity, piecewise-linear, strain-hardening, isotropic

20. ABSTRACT (Continue on reverse side if necessary and identify by block number)

A 20-faced polyhedron is chosen as a reasonable piecewise linear approximation to either the Mises or Tresca yield criterion. Strain hardening and motion of the faces during hardening are assumed to be linear functions. Subject to the above assumptions, to initial isotropy, and to some reasonable symmetry requirements it is shown that the most general possible theory contains 11 material constants. Some simple experiments with a thin-walled tube are suggested for determining these constants.

DD FORM 1 JAN 73 1473 EDITION OF 1 NOV 65 IS OBSOLETE S/N 0102-014-6601 | SECURITY CLASSIFICATION OF THIS PAGE (When Data Entered)

405 395

A PIECEWISE LINEAR THEORY OF PLASTICITY FOR AN INITIALLY ISOTROPIC MATERIAL IN PLANE STRESS

by

Philip G. Hodge, Jr.

Abstract

A 20-faced polyhedron is chosen as a reasonable piecewise linear approximation to either the Mises or Tresca yield criterion. Strain hardening and motion of the faces during hardening are assumed to be linear functions. Subject to the above assumptions, to initial isotropy, and to some reasonable symmetry requirements it is shown that the most general possible theory contains 11 material constants. Some simple experiments with a thin-walled tube are suggested for determining these constants.

A PIECEWISE LINEAR THEORY OF PLASTICITY FOR AN INITIALLY ISOTROPIC MATERIAL IN PLANE STRESS

by

Philip G. Hodge, Jr.

1. Introduction. Plastic behavior is an essentially nonlinear phenomenon, even in the range of small strains. There are three aspects to this nonlinear behavior: the initial yield condition, the hardening characteristics or stress-strain curve, and the change of yield condition with hardening. Any nonlinear behavior can be approximated by a collection of linear elements, and there are obvious conceptual and computational advantages to the resulting piecewise linear theory. In the present paper we shall adopt a restrictive definition "piecewise linear" in that the stress-strain curve is to be approximated with a bilinear curve with one elastic and one plastic slope. Further, although the yield condition may have any number of linear pieces, the change in position of any piece due to the stress-point on any particular other piece will have a single linear expression.

As implied by the title, we consider only a material which is initially isotropic. However, there is an essential internal contradiction between the terms linear (or piecewise linear) and isotropic. If the yield condition is expressed in the form $f(\sigma) = 0$ in one coordinate system x then, for an isotropic material, f will necessarily have the same form in any other coordinate system $\bar{x}$. This restriction greatly limits the functional form of f, and, in particular, rules out all linear functions.

In earlier work on this subject [1-3]*, attention was limited to situations in which the principal directions were known and fixed at each point, so that there was no occasion to introduce a coordinate transformation and the problem did not arise.

In Sec. 2 we discuss this point further. We take the approach that the coordinate directions at each point may be chosen arbitrarily, but once chosen they must remain fixed. From the viewpoint that any piecewise linear condition is an approximation to the "true" yield condition, a different choice of coordinate axes simply constitutes a different approximation to reality.

Our basic interest in this paper is in problems of plane stress where in some direction x_3, $\sigma_{13} = \sigma_{23} = \sigma_{33} = 0$. However, since plastic behavior is independent of mean normal stress, all plastic results will remain the same if any values $\sigma_{11} = \sigma_{22} = \sigma_{33}$ are added. Therefore, in order to more clearly see the symmetries of the problem, we will consider a generalized stress vector $\underset{\sim}{\sigma}^*$ with four components

$$\underset{\sim}{\sigma}^* = (\sigma_{11}, \sigma_{22}, \sigma_{33}, \tau_{12}) \tag{1}$$

and a corresponding generalized strain vector

$$\underset{\sim}{\varepsilon} = (\varepsilon_{11}, \varepsilon_{22}, \varepsilon_{33}, \gamma_{12}) \tag{2}$$

For most of the paper we will find it convenient to use a dimensionless generalized stress

$$\underset{\sim}{\sigma} = \underset{\sim}{\sigma}^*/\sigma_0 = (\sigma_1, \sigma_2, \sigma_3, \tau) \tag{3}$$

*Numbers in brackets refer to the references collected at the end of the paper.

where σ_0 is the initial tensile yield stress, and to deal with the plastic strain rate

$$\dot{\underset{\sim}{\varepsilon}}^P = (\dot{\varepsilon}_1, \dot{\varepsilon}_2, \dot{\varepsilon}_3, \dot{\gamma}) \tag{4}$$

Equations (2) and (4) are, of course, related by

$$\dot{\underset{\sim}{\varepsilon}} = \dot{\underset{\sim}{\varepsilon}}^e + \dot{\underset{\sim}{\varepsilon}}^P \tag{5}$$

where $\dot{\underset{\sim}{\varepsilon}}^e$ is given in terms of stress rates by Hooke's law.

As previously mentioned, Sec. 2 will be concerned with the piecewise-linear approximation to the yield surface. We shall choose a particular 20-sided yield polyhedron and show that the approximation is not unduly sensitive to different choices of axes. Once the piecewise-linear yield condition has been chosen, our approach will be to construct the most general piecewise-linear theory which can be associated with it, subject to the restriction of initial isotropy and some plausible symmetry requirements.

Hardening laws will be developed in Sec. 3. Initial isotropy demands that a single material constant be sufficient to define hardening for all faces of the yield polygon, but several additional material constants may be introduced to define the most general admissible laws for a stress point on an edge or corner.

The next two sections are concerned with possible changes in the yield condition due to hardening. Beginning with the most general linear motions of the individual sides, we show that constraints of initial isotropy, reasonable symmetry, and restriction to a 20-sided yield polyhedron lead eventually to a theory with only eight plastic constants. Specifically, Sec. 4

considers face motions due to the stress point on a face, and in Sec. 5 we derive certain necessary inequalities on the eight plastic constants. In an appendix, we show that nothing more is required to define the face motions when the stress point is in an edge or corner.

The next brief section restates the results in terms appropriate to a thin-walled tube under an arbitrary history of axial tension, internal pressure, and twist. Elastic effects are included and all quantities have proper physical dimensions.

In Sec. 7 we outline a series of experiments on thin-walled tubes to determine the 11 constants (two elastic constants, initial yield stress, and eight plastic constants) required by the theory. Most of the constants are determined by one test and checked by an independent one to provide some feeling for the adequacy of the theory.

The paper closes with some general remarks relating the proposed theory with the existing state of knowledge of plastic strain hardening.

2. Initial yield condition. Let the z-direction permanently be in the favored direction appropriate to plane stress so that $\sigma_z = \tau_{xz} = \tau_{yz} = 0$, and let the x and y-directions be arbitrary but fixed. Then the Mises [4] and Tresca [5] yield conditions may be written, respectively as:

$$\sigma_x^2 - \sigma_x\sigma_y + \sigma_y^2 + 3\tau_{xy}^2 = \sigma_0^2 \qquad (6a)$$

$$\max\left[\left|\frac{\sigma_x+\sigma_y}{2}\right| + \sqrt{\left(\frac{\sigma_x-\sigma_y}{2}\right)^2 + \tau_{xy}^2},\ 2\sqrt{\left(\frac{\sigma_x-\sigma_y}{2}\right)^2 + \tau_{xy}^2}\right] = \sigma_0 \qquad (6b)$$

The solid lines in Fig. 1 show these yield conditions for three important special cases. Since both yield conditions are isotropic, Eqs. (6) and the solid curves in Fig. 1 would be exactly the same if x, y were to be replaced by any other orthogonal axes $\bar{x}$, $\bar{y}$.

As a piecewise linear (PWL) approximation to either of equations 6 we define a surface with 24 vertices, 42 edges, and 20 faces as shown in Fig. 2 and defined in Table 1. Typical equations for the faces are

$$\begin{aligned}
&X,\ X': && \pm 2\tau_{xy} = \sigma_0 \\
&Y_{AB},\ Y'_{AB}: && (2/7)[3\sigma_x \pm 4\tau_{xy}] = \sigma_0 \\
&Y_{FA},\ Y'_{FA}: && (2/7)[3(\sigma_x - \sigma_y) \pm 4\tau_{xy}] = \sigma_0 \qquad (7) \\
&Z_{AB}: && \sigma_x = \sigma_0 \\
&Z_{FA}: && \sigma_x - \sigma_y = \sigma_0
\end{aligned}$$

It is difficult to picture the comparison of the PWL condition with the Mises or Tresca ones in the three-dimensional stress space of Fig. 2, so we will restrict graphical comparison to the three special cases of Fig. 1. In biaxial tension with $\tau_{xy} = 0$, (Fig. 1a) the PWL and Tresca curves are identical, but in uniaxial (Fig. 1b) or equal biaxial (Fig. 1c) tension vs. torsion the PWL curve is shown by a heavy dashed line. As the figures show it is a rather close approximation to either the Tresca or Mises condition, but cannot be characterized as internal or external to either of them.

Let the material be referred to a different set of axes $\bar{x}$, $\bar{y}$. The stress components in the different coordinates would be related by the well-known formulas

$$\sigma_x = \tfrac{1}{2}(\bar{\sigma}_x + \bar{\sigma}_y) + \tfrac{1}{2}(\bar{\sigma}_x - \bar{\sigma}_y)\cos 2\phi - \bar{\tau}_{xy} \sin 2\phi$$

$$\sigma_y = \tfrac{1}{2}(\bar{\sigma}_x + \bar{\sigma}_y) - \tfrac{1}{2}(\bar{\sigma}_x - \bar{\sigma}_y)\cos 2\phi + \bar{\tau}_{xy} \sin 2\phi \qquad (8)$$

$$\tau_{xy} = \tfrac{1}{2}(\bar{\sigma}_x - \bar{\sigma}_y)\sin 2\phi + \bar{\tau}_{xy} \cos 2\phi$$

where ϕ is the angle from x to $\bar{x}$. If (8) is substituted in either of (6), ϕ will drop out and the equation will have the identical form in terms of the barred stresses. However, the substitution of (8) in any of (7) will lead to a different form of equation which depends upon ϕ. The three remaining curves in Fig. 1 show the resulting yield polygons for three particular values of ϕ.

As an example of the significance of these curves, consider the long-dashed polygon in Fig. 1a, corresponding to $\cos 2\phi = 0.8$ ($\sin 2\phi = 0.6$). Suppose that the true yield behavior of the material is governed by the PWL condition with reference to the x, y axes. Then, an experiment with $\tau_{xy} = 0$ would lead to the heavy solid curve in Fig. 1a. In terms of Fig. 2, this curve would be on the faces $Z_{AB} - Z_{BC} - \ldots - Z_{FA}$ and its vertices would be the midpoints of sides A_2A_2', B_2B_2', etc.

Consider now a second experiment on the same material with $\bar{\tau}_{xy} = 0$. For the particular ϕ considered, Eqs. (8) would become

$$\sigma_x = 0.9\bar{\sigma}_x + 0.1\bar{\sigma}_y, \quad \sigma_y = 0.1\bar{\sigma}_x + 0.9\bar{\sigma}_y, \quad \tau_{xy} = 0.3(\bar{\sigma}_x - \bar{\sigma}_y) \qquad (9)$$

In particular, for $\bar{\sigma}_y = 0$, $\tau_{xy} = 0.3\bar{\sigma}_x$ would apparently be greater than $\sigma_0/8$. The yield point in Fig. 2 would thus be on line A_1A_2 rather than A_2A_2'. Continuing this reasoning it appears (and is retroactively verified) that the resulting polygon would lie on sides $Y_{AB} - Z_{AB} - Z_{BC} - Y'_{BC} - Y'_{CD} - Y'_{DE} - Z_{DE} - Z_{EF} - Y_{EF} - Y_{FA} - Y_{AB}$ in Fig. 2. The coordinates of the vertices are now easily found, and converted into the $\bar{x}$, $\bar{y}$ system by the inverses of Eqs. (9), resulting in the long-dashed curve in Fig. 1a.

Now, in solving a problem using the PWL condition, we will use the heavy dashed curve corresponding to the x, y axes. If the "true" PWL corresponds to some other set of axes, we are approximating one of the light broken-line polygons in Fig. 1 by the heavy one. Figure 1 shows clearly that any of these approximations are of the same order as the original approximation of the Tresca or Mises condition by the PWL one.

For example, if a finite-element model is used to solve a particular problem one might either base the PWL condition on fixed x, y axes throughout the domain, or on a different set of local axes for each element. Figure 1 shows that the discrepancy between these two solutions would be comparable between to that between either of them and the true Tresca or Mises conditions - or to that between the Tresca and Mises. In other words, the error introduced by the fact that the PWL condition is not isotropic is no greater than that introduced by approximating the Tresca condition for the Mises one.

3. Hardening laws. In this and the next three sections we consider the relation between the stress rates, plastic strain

rates, and changes in the yield conditions using the notation of Eqs. (3) and (4). We assume the plastic potential flow law [6] with linear hardening when the stress point is on a single face. Thus

$$\dot{\underset{\sim}{\varepsilon}}^p \equiv (\dot{\varepsilon}_1, \dot{\varepsilon}_2, \dot{\varepsilon}_3, \dot{\gamma}) = (\dot{f}/B)\ \partial f/\partial \underset{\sim}{\sigma} \qquad (10)$$

where $f = \sigma_0$ is the equation of the appropriate one of the twenty faces. In view of the assumed initial isotropy, the hardening constant B is the same for each face. Representative specific forms of (10) are

$$X: \quad B\dot{\underset{\sim}{\varepsilon}}^p = 4\,\dot{\tau}(0,\ 0,\ 0,\ 1) \qquad (11a)$$

$$Y_{AB}: \quad B\dot{\underset{\sim}{\varepsilon}}^p = (4/49)[3(\dot{\sigma}_1 - \dot{\sigma}_3) + 4\dot{\tau}](3,0,\ -3,4) \qquad (11b)$$

$$Z_{AB}: \quad B\dot{\underset{\sim}{\varepsilon}}^p = (\dot{\sigma}_1 - \dot{\sigma}_3)(1,\ 0,\ -1,0) \qquad (11c)$$

Notice that in all cases the incompressibility requirement $\dot{\varepsilon}_1 + \dot{\varepsilon}_2 + \dot{\varepsilon}_3 = 0$ is automatically satisfied.

Consider next the case where the stress point is on an edge and remains there. There will be one normality constraint, hence there should be two actual relations between stress rate and plastic strain rate. For example, on edge A_2B_2 between faces Y_{AB} and Z_{AB}, normality demands that

$$\dot{\varepsilon}_2 = 0 \qquad (12a)$$

Incompressibility then demands that $\dot{\varepsilon}_3 = -\dot{\varepsilon}_1$, so that we may write the most general linear relations in terms of four constants P_i:

$$\dot{\sigma}_1 - \dot{\sigma}_3 = P_1\dot{\varepsilon}_1 + P_2\dot{\gamma} \qquad \dot{\tau} = P_3\dot{\varepsilon}_1 + P_4\dot{\gamma} \qquad (12b,c)$$

Now Z_{AB} is a special case of edge A_2B_2, defined by $\dot{\gamma} = 0$.

Comparison of (12b) and (11c) then shows that $p_1 = B$. Similarly, the special case Y_{AB} leads to the relation $13B = 16(3p_2 + 3p_3 + 4p_4)$. Defining new constants* $C = 8p_2$ and $g = 8p_3$ we can rewrite Eqs. (12) as

$$A_2B_2: \quad \dot{\varepsilon}_2 = 0 \qquad \dot{\sigma}_1 - \dot{\sigma}_3 = B\dot{\varepsilon}_1 + (1/8)C\dot{\gamma}$$

$$\dot{\tau} = (g/8)\,\dot{\varepsilon}_1 + [(13/64)B - 3(C+g)/32]\dot{\gamma} \qquad (13)$$

In view of the assumed initial isotropy, the laws for edges $B_2C_2,\ldots,F_2A_2$ may be obtained from (13) by an appropriate change of subscripts and no new constants will be introduced. Finally, we note that Eqs. (13) may be inverted and solved for the strain rates:

$$\dot{\varepsilon}_1 = -\dot{\varepsilon}_3 = \frac{1}{\Delta_1}\left[\left(\frac{13}{64}B - 3\frac{C+g}{32}\right)(\dot{\sigma}_1 - \dot{\sigma}_3) - \frac{1}{8}C\dot{\tau}\right] \qquad \dot{\varepsilon}_2 = 0$$

$$\dot{\gamma} = \frac{1}{\Delta_1}\left[-\frac{1}{8}g(\dot{\sigma}_1 - \dot{\sigma}_3) + B\dot{\tau}\right] \qquad \Delta_1 = \frac{13}{64}B^2 - 3B\frac{C+g}{32} - \frac{Cg}{64} \qquad (14)$$

The other edges may be treated in similar fashion with the following typical results:

$$B_2B_3': \quad \dot{\gamma} = 0 \qquad \dot{\sigma}_1 - \dot{\sigma}_3 = B\dot{\varepsilon}_1 + A\dot{\varepsilon}_2$$

$$\dot{\sigma}_2 - \dot{\sigma}_3 = A\dot{\varepsilon}_1 + B\dot{\varepsilon}_2 \qquad (15)$$

$$B_1B_2: \quad \dot{\gamma} = (4/3)(\dot{\varepsilon}_1 + \dot{\varepsilon}_2)$$

$$3(\dot{\sigma}_1 - \dot{\sigma}_3) + 4\dot{\tau} = (1/12)(49B\dot{\varepsilon}_1 + c\dot{\varepsilon}_2)$$

---

*Throughout this section we shall use capital letters to denote constants which will be part of the final PWL model, and lower case letters for constants which will be reassigned during further development. The final form of the equations are summarized in Table 2.

$$3(\dot{\sigma}_2 - \dot{\sigma}_3) + 4\dot{\tau} = (1/12)(c\dot{\varepsilon}_1 + 49B\dot{\varepsilon}_2) \qquad (16)$$

A_1B_1: $\dot{\varepsilon}_2 = 0 \qquad \dot{\tau} = (1/4)(h\dot{\varepsilon}_1 + B\dot{\gamma})$

$$\dot{\sigma}_1 - \dot{\sigma}_3 = (1/12)[11B - 4(D+h)]\dot{\varepsilon}_1 + (D/4)\dot{\gamma} \qquad (17)$$

Edges such as C_1C_2 are obtained by appropriate subscript changes in Eq. (16), etc., and edges such as $B_1'B_2'$ are obtained by changing the signs of $\dot{\tau}$ and $\dot{\gamma}$ in Eq. (16), etc. Therefore, we now have all the face and side flow laws in terms of the seven constants A, B, C, D, c, g, and h.

Finally, if the stress point is in a corner and remains there, there will be no normality condition and three flow laws. Because of the symmetry between 1 and 2, the most general linear law for corner B_2 can be written in terms of 5 constants

$$\dot{\sigma}_1 - \dot{\sigma}_3 = P_1\dot{\varepsilon}_1 + P_2\dot{\varepsilon}_2 + P_3\dot{\gamma} \qquad (18a)$$

$$\dot{\sigma}_2 - \dot{\sigma}_3 = P_2\dot{\varepsilon}_1 + P_1\dot{\varepsilon}_2 + P_3\dot{\gamma} \qquad (18b)$$

$$\dot{\tau} = P_4\dot{\varepsilon}_1 + P_4\dot{\varepsilon}_2 + P_5\dot{\gamma} \qquad (18c)$$

Now edge B_2B_2' is a special case of corner B_2, so that when $\dot{\gamma} = 0$, Eqs. (18a,b) must reduce to Eqs. (15), whence $P_1 = B$ and $P_2 = A$. Similar consideration of the special case of A_2B_2 ($\dot{\varepsilon}_2 = 0$) shows that $P_3 = C/8$, $P_4 = g/8$, and $P_5 = [13B-6(C+g)]/64$, so that all five P_i are defined in terms of the constants we have already introduced. When we now demand that the special case $3\dot{\gamma} = 4(\dot{\varepsilon}_1 + \dot{\varepsilon}_2)$ corresponding to edge B_1B_2 agree with Eq. (16) we are led to the two different expressions

$$12[3(\dot{\sigma}_1 - \dot{\sigma}_3) + 4\dot{\tau}] = 49B\dot{\varepsilon}_1 + (36A + 13B)\dot{\varepsilon}_2$$
$$= 49B\dot{\varepsilon}_1 + c\dot{\varepsilon}_2 \qquad (19)$$

which can be an identity only if

$$c = 36A + 13B \qquad (20)$$

Thus we see that proper consideration of the corner flow law reduces the number of available constants, and Eqs. (18) can be written

$$B_2: \quad \dot{\sigma}_1 - \dot{\sigma}_3 = B\dot{\varepsilon}_1 + A\dot{\varepsilon}_2 + (C/8)\dot{\gamma}$$
$$\dot{\sigma}_2 - \dot{\sigma}_3 = A\dot{\varepsilon}_1 + B\dot{\varepsilon}_2 + C/8)\dot{\gamma}$$
$$\dot{\tau} = (g/8)(\dot{\varepsilon}_1 + \dot{\varepsilon}_2) + [13B - 6(C+g)]\dot{\gamma}/64 \qquad (21)$$

A similar treatment of corner B_1 leads to

$$B_1: \quad \dot{\sigma}_1 - \dot{\sigma}_3 = [A - B/12 - (D+h)/3]\dot{\varepsilon}_1$$
$$+ [11B/12 - (D+h)/3] \quad \dot{\varepsilon}_2 + D\dot{\gamma}/4$$
$$\dot{\sigma}_2 - \dot{\sigma}_3 = [11B/12 - (D+h)/3]\dot{\varepsilon}_1$$
$$+[A-B/12 - (D+h)/3] \quad \dot{\varepsilon}_2 + D\dot{\gamma}/4$$

$$\dot{\tau} = (h/4)(\dot{\varepsilon}_1 + \dot{\varepsilon}_2) + B\dot{\gamma}/4 \qquad (22)$$

where we have added neither constants nor constraints.

4. Change of yield condition. We begin with the general assumption that each face moves only in translation and does not rotate. Therefore, when the stress point has a given motion such that it remains on a given face α, the change in the yield condition is fully defined by the 20 numbers $\dot{f}_\beta$ for the 20 different faces. The number $\dot{f}_\alpha$ is determined by the fact that the stress point remains on face α and hence may be taken as known. For any other face β, let

$$\dot{f}_\beta = (1/B)\phi(\alpha,\beta)\dot{f}_\alpha \tag{23}$$

Then $\phi(\alpha,\alpha) = B$ and it remains to define the remaining 380 members of the 20 x 20 matrix $\phi(\alpha,\beta)$.

We make the reasonable requirement that ϕ is symmetric and call frequently on the original isotropy of the material. Consider first the case where the stress point is on face X, i.e., $\alpha = X$. Then without loss of generality we may take

$$\dot{f}_\alpha = 2\dot{\tau} = (1/2)B\dot{\gamma} = 1$$
$$\dot{\epsilon}_1 = \dot{\epsilon}_2 = \dot{\epsilon}_3 = 0 \tag{24}$$

Now, a special case of face X is the corner B_1. Substitution of (24) in (22) shows that the stress point moves according to

$$\dot{\sigma}_1 - \dot{\sigma}_3 = \dot{\sigma}_2 - \dot{\sigma}_3 = D/2B \qquad \dot{\tau} = 1/2 \tag{25}$$

But during this motion, face Y_{AB} must move so that it stays attached to corner B_1, so that $\dot{f}_{YAB}$ must also be governed by (25). Thus,

$$\dot{f}_{YAB} = (2/7)[3(\dot{\sigma}_1 - \dot{\sigma}_3) + 4\dot{\tau}] = (1/7B)(3D+4B) \tag{26}$$

Substitution of (26) and (24) in (23) then shows that

$$\phi(X, Y_{AB}) = (3D + 4B)/7 \tag{27}$$

Initial isotropy or a repetition of the above argument shows that $\phi(X, Y_{ij})$ is given by (27) for all six of the faces adjoining face X.

Since face X does not adjoin any of the other faces, we cannot deduce any further information, but must introduce new constants to describe the motion of the remaining faces. However, initial isotropy dictates that only three new constants

are necessary:

$$\phi(X, Z_{ij}) = G \qquad \phi(X, Y'_{ij}) = H \qquad \phi(X,X') = I \tag{28}$$

The results to date are summarized in the X column of Table 3. All $\phi(X',\beta)$ are of course, easily expressed in terms of the same constants.

We consider next the case where the stress point is on face Y_{AB}. Setting $\dot{f}_{YAB} = 1$ it follows from (11b) that

$$\dot{\epsilon}_1 = -\dot{\epsilon}_3 = (6/7)B \qquad \dot{\epsilon}_2 = 0 \qquad \dot{\gamma} = (8/7)B \tag{29}$$

If the stress point stays at the particular point B_1 of face Y_{AB}, Eqs. (22) and (29) show that its motion is

$$\dot{\sigma}_1 - \dot{\sigma}_3 = (11B - 4h)/14B$$
$$\dot{\sigma}_2 - \dot{\sigma}_3 = (12A - B - 4h)/14B$$
$$\dot{\tau} = (4B + 3h)/14B \tag{30}$$

Therefore if face X is to remain attached to B_1,

$$\dot{f}_X = 2\dot{\tau} = (4B + 3h)/7B \tag{31}$$

whence

$$\phi(Y_{AB},X) = (4B + 3h)/7 \tag{32}$$

Comparison of (32) and (27) and symmetry of ϕ then shows that

$$h = D \tag{33}$$

Now corner B_1 must also remain attached to face Y_{BC} whence

$$\dot{f}_{YBC} = (2/7)[3(\dot{\sigma}_2 - \dot{\sigma}_3) + 4\dot{\tau}] = (36A + 13B)/49B \tag{34}$$

Further, symmetry demands that $\dot{f}_{YFA}$ has the same value so that we obtain

$$\phi(Y_{AB}, Y_{BC}) = \phi(Y_{AB}, Y_{FA}) = (36A + 13B)/49 \tag{35}$$

Face Y_{AB} does not adjoin the other Y faces so that we need two new constants.

$$\phi(Y_{AB}, Y_{CD}) = \phi(Y_{AB}, Y_{EF}) = k \tag{36a}$$

$$\phi(Y_{AB}, Y_{DE}) = j \tag{36b}$$

A similar analysis with regard to corner B_2 and faces Z_{AB} and Z_{BC} shows that

$$\phi(Y_{AB}, Z_{AB}) = (6B + C)/7 \tag{36c}$$

$$\phi(Y_{AB}, Z_{BC}) = \phi(Y_{AB}, Z_{FA}) = (6A + C)/7 \tag{36d}$$

Since face Y_{AB} does not adjoin any other faces, we must introduce several additional constants:

$$\phi(Y_{AB}, Z_{CD}) = \phi(Y_{AB}, Z_{EF}) = \ell \tag{36e}$$

$$\phi(Y_{AB}, Z_{DE}) = m \qquad \phi(Y_{AB}, Y'_{AB}) = p \tag{36f,g}$$

$$\phi(Y_{AB}, Y'_{BC}) = \phi(Y_{AB}, Y'_{FA}) = q \tag{36h}$$

$$\phi(Y_{AB}, Y'_{CD}) = \phi(Y_{AB}, Y'_{EF}) = r \tag{36i}$$

For face Y'_{DE} we note that initial isotropy demands that the motion of the face opposite the stress point should be the same for all faces, hence

$$\phi(Y_{AB}, Y'_{DE}) = \phi(X,X') = I \tag{36j}$$

Finally, for face X' we use isotropy and symmetry to conclude

$$\phi(Y_{AB}, X') = \phi(X', Y_{AB}) = \phi(X, Y'_{AB}) = H \tag{36k}$$

All other $\phi(Y_{ij}, \beta)$ and all $\phi(Y'_{ij}, \beta)$ may, of course, be obtained by suitable interchanges of subscripts.

Finally, we consider the stress point on side Z_{AB} with

$$\dot{f}_{ZAB} = \dot{\sigma}_1 - \dot{\sigma}_3 = 1 \qquad \dot{\varepsilon}_1 = -\dot{\varepsilon}_3 = 1/B \qquad \dot{\gamma} = 0 \tag{37}$$

For the particular point B_2 we obtain

$$\dot{\sigma}_1 - \dot{\sigma}_3 = 1 \qquad \dot{\sigma}_2 - \dot{\sigma}_3 = A/B \qquad \dot{\tau} = g/8B \tag{38}$$

whence

$$\dot{f}_{YAB} = (2/7)[3(\dot{\sigma}_1 - \dot{\sigma}_3) + 4\dot{\tau}] = (6B + g)/7B \tag{39}$$

Comparison with (36c) and symmetry of ϕ then shows that

$$g = C \tag{40}$$

In Table 2 we have summarized the flow laws derived in Sec. 3 and simplified by Eqs. (20), (33), and (40).

Next, the requirement that Z_{BC} remain attached to B_2 leads to

$$\phi(Z_{AB}, Z_{BC}) = \phi(Z_{AB}, Z_{FA}) = A \tag{41a}$$

We introduce one new constant and complete the description of the motion with

$$\phi(Z_{AB}, Z_{CD}) = \phi(Z_{AB}, Z_{EF}) = J \tag{41b}$$

$$\phi(Z_{AB}, Z_{DE}) = I \tag{41c}$$

All remaining terms of the ϕ matrix are given by symmetry and suitable interchanges of indices.

The number of arbitrary constants introduced above is significantly reduced by the requirement that no new sides be introduced. Corner B_1 is at the intersection of three planes and hence is uniquely defined for any translational motion of those planes. However, B_2 is at the intersection of four planes. Therefore, if it is to be uniquely defined (the alternative

would be the creation of a new plane) the four planes whose motions are given by

$$\dot{f}_{ZAB} = \dot{\sigma}_1 - \dot{\sigma}_3 \qquad \dot{f}_{YAB} = (2/7)[3(\dot{\sigma}_1 - \dot{\sigma}_3) + 4\dot{\tau}] \tag{42}$$

$$\dot{f}_{ZBC} = \dot{\sigma}_2 - \dot{\sigma}_3 \qquad \dot{f}_{YBC} = (2/7)[3(\dot{\sigma}_2 - \dot{\sigma}_3) + 4\dot{\tau}]$$

must continue to intersect at a point. In other words, since the four numbers f in (42) are defined by only three parameters $\dot{\sigma}_1 - \dot{\sigma}_3$, $\dot{\sigma}_2 - \dot{\sigma}_3$, and $\dot{\tau}$, they must satisfy the constraint

$$6(\dot{f}_{ZAB} - \dot{f}_{ZBC}) = 7(\dot{f}_{YAB} - \dot{f}_{YBC}) \tag{43}$$

This constraint must hold for the stress point on any face α, hence the $\phi(\alpha,\beta)$ defined previously must satisfy

$$6[\phi(\alpha,Z_{AB}) - \phi(\alpha,Z_{BC})] = 7[\phi(\alpha,Y_{AB}) - \phi(\alpha,Y_{BC}) \tag{44}$$

When $\alpha = X$, Eq. (44) reduces to

$$6(G-G) = (3D + 4B) - (3D + 4B) \tag{45}$$

which is identically satisfied, and the same result holds for $\alpha = Y_{AB}$, $\alpha = Z_{AB}$, and $\alpha = X'$. However, setting $\alpha = Y_{BC}$ and using the symmetry of ϕ we obtain

$$\alpha = Y_{BC}: \quad (6/7)(6A + C - 7\ell) = (1/7)(36A + 13B - 49k) \tag{46}$$

When all faces α are considered, we obtain a total of seven independent constraints which are sufficient to determine the seven remaining constants denoted with lower case letters:

$$\ell = (C + 6J)/7 \qquad m = (C + 6I)/7$$
$$k = (36J + 13B)/49 \qquad j = (36I + 13B)/49 \tag{47}$$
$$r = (36J + 13I)/49 \qquad q = (36A + 13I)/49$$
$$p = (36B + 13I)/49$$

The complete results for $\phi(\alpha,\beta)$ are conveniently summarized in Table 3.

If the stress point is in an edge or corner, the motion of all sides may be deduced from the concept of artificial stress points [2,3] on the adjacent sides with the same total effect. Some details of this method are given in an Appendix, and the results are summarized in Table 4.

5. Transitions. When the stress point is on an edge, it may move so as to stay on the edge or it may move off into one of the adjacent faces. The inequalities that govern this choice are easily determined.

For example, consider a stress point S on edge A_1B_1 which is just on the verge of moving to face X. Then the flow laws of both the edge and face must apply, hence, from Table 2,

$$\dot{\varepsilon}_1 = \dot{\varepsilon}_2 = \dot{\varepsilon}_3 = 0 \qquad \dot{\gamma} = (4/B)\dot{\tau} = (4/D)(\dot{\sigma}_1 - \dot{\sigma}_3) \tag{48}$$

It is clear from Fig. 2 that $\dot{\gamma}$, $\dot{\tau}$, and $(\dot{\sigma}_1 - \dot{\sigma}_3)$ are all non-negative under these circumstances, hence B and D are both non-negative. Also, for a given $\dot{\sigma}_1 - \dot{\sigma}_3$ it is clear that S will move onto side X if $\dot{\tau}$ is sufficiently large. Therefore, the condition that S move onto face X is

$$X(A_1B_1): \quad \dot{\tau}/(\dot{\sigma}_1 - \dot{\sigma}_3) \geq B/D \tag{49a}$$

Similarly, if S is on A_1B_1 but on the verge of moving onto Y_{AB}, it is easy to show that 11B-4D is non-negative and that

$$Y_{AB}(A_1B_1): \quad \dot{\tau}/(\dot{\sigma}_1 - \dot{\sigma}_3) \leq (3D+4B)/(11B-4D) \tag{49b}$$

Therefore, S will remain on A_1B_1 if and only if both inequalities (49) are violated, i.e., if

$$A_1B_1: \quad \frac{3D+4B}{11B-4D} \leq \frac{\dot{\tau}}{\dot{\sigma}_1 - \dot{\sigma}_3} \leq \frac{B}{D} \tag{50}$$

We introduce the reasonable requirement that there be at least one motion of S which remains on A_1B_1, whence the left-hand side cannot exceed the right-hand side of (50). Together with our earlier observations, this requirement leads to the restrictions

$$0 \leq D \leq B \tag{51a}$$

The other edges may be treated in similar fashion to deduce the further restrictions on the hardening constants

$$0 \leq C \leq B \qquad 0 \leq A \leq B \tag{51b,c}$$

The resulting inequalities governing the motion of S are summarized in Table 4a which is to be interpreted as follows: when S is on a given edge it will remain on that edge if both inequalities in that line are satisfied, and it will move to the face listed at the left (right) if the left (right) inequality is violated.

When S is in a corner, it may remain there or move to an adjacent edge or face. Consider a stress point in corner B_2 and incipiently moving to edge B_1B_2. Then both sets of laws in Table 2 must apply hence,

$$\frac{16\dot{\tau}}{13B-6C} = \frac{\dot{\varepsilon}_1+\dot{\varepsilon}_2}{3} = \frac{\dot{\sigma}_1+\dot{\sigma}_2-2\dot{\sigma}_3}{3A+3B+C} \tag{52}$$

Evidently S will remain in B_2 if the left member of (52) is less than the right, and move onto B_1B_2 if it is greater.

Inequalities governing motion between B_2 and the edges $B_2'B_2$, C_2B_2, and B_2A_2 are obtained similarly, as are those between B_1 and its three edges. Table 4b summarizes the results. S will remain on B_2 if and only if all four inequalities in the

the last two lines are satisfied; if exactly one inequality is violated, it will move onto the corresponding edge; if two inequalities are simultaneously violated, it will move onto the face determined by those two edges. A similar interpretation applies to the first two lines of Table 4b and motion of a stress point on corner B_1.

Finally we note that if the hardening constants satisfy (51), the domain of each corner will be non-void so that no new constraints are introduced.

6. Thin tube. We consider a closed thin circular cylinder of length L, radius a, and thickness h under a positive internal pressure p, a twisting moment M in either direction, and a positive or negative axial force F.

We choose cylindrical coordinates $x_1 = \theta$, $x_2 = z$, $x_3 = r$ and assume that $\sigma_r = \tau_{r\theta} = \tau_{rz} = 0$ in a state of plane stress. The remaining stresses are given by

$$\sigma_\theta = pa/h \qquad \tau_{\theta z} = M/2\pi a^2 h \tag{53}$$

$$\sigma_z = F/2\pi ah + pa/2h$$

The simplicity of Eqs. (53) entitles us to regard the stress as directly controllable and measurable, subject only to $\sigma_\theta \geq 0$.

Let u be the increase in radius, w the increase in length, and v the relative tangential displacement between the two ends. Then the strains are

$$\varepsilon_\theta = u/a \qquad \varepsilon_z = w/L \qquad \gamma = v/L \tag{54}$$

Again, the simplicity of (54) enables us to regard the strains as directly measurable.

For an isotropic material in plane stress the elastic strain rates are

$$\dot{\varepsilon}_\theta^e = (\dot{\sigma}_\theta - \nu\dot{\sigma}_z)/E \qquad \dot{\varepsilon}_z^e = (\dot{\sigma}_z - \nu\dot{\sigma}_\theta)/E \tag{55a,b}$$

$$\dot{\gamma}^e = 2(1+\nu)\dot{\tau}_{\theta z}/E \tag{55c}$$

The initial yield condition is shown in Fig. 2 and Table 1 with the alternate labels for the axes.

The constitutive equations are appropriate combinations of Eqs. (55) and Table 3. As an example, on face X, Eqs. (55a,b) continue to hold with (55c) replaced by

$$X: \quad \dot{\gamma} = \left[\frac{2(1+\nu)}{E} + \frac{4}{B}\right]\dot{\tau}_{\theta z} \tag{56}$$

Similarly, on face Y_{AB}, the equations are (55b) together with

$$Y_{AB}: \quad \dot{\varepsilon}_\theta = (\dot{\sigma}_\theta - \nu\dot{\sigma}_z)/E + (12/49B)(3\dot{\sigma}_\theta + 4\dot{\tau}_{\theta z}) \tag{57}$$

$$\dot{\gamma} = (2/E)(1+\nu)\dot{\tau}_{\theta z} + (16/49B)(3\dot{\sigma}_\theta + 4\dot{\tau}_{\theta z})$$

As a final example, on face Z_{BC} we retain (55a,c) and add

$$Z_{AB}: \quad \dot{\varepsilon}_z = (\dot{\sigma}_z - \nu\dot{\sigma}_\theta)/E + \dot{\sigma}_z/B \tag{58}$$

7. Determination of constants. We consider a series of possible experiments on the thin-walled tube of the previous section in order to determine the 11 material constants (E, ν, σ_0, A,B,C,D,G,H,I,J) of the PWL model. Experimental data, will of course, result in a set of points with measured coordinates. If more than two points are used, they will not, in general, fall exactly on a straight line as assumed by our model. Therefore, the first step in the analysis will be to approximate their true locus by a straight line. The accuracy of this approximation will, of course, be one indication of the appropriateness of the theory. From here on we shall assume that this approximation has been made and is appropriate. For simplicity of exposition, then, we shall regard the resulting lines as direct results of the experiments.

The general pattern of all of the tests will consist of four phases. We first load elastically until the stress point S touches one face α on the initial yield surface, then continue to load a small amount plastically with S remaining on α to a final position S_1. In phase 3 we unload elastically to some convenient interior point. Finally, phase 4 reloads in some different direction until S just touches a different face β. Phases 1 and 2 of any test will determine E, σ_0, B, and (for most tests) ν. Measurements from different tests will help assess the validity of this phase of the PWL model.

During phase 2, face β will move according to Eq. (23). Using the initial value of σ_0 for each face, we can integrate and solve for ϕ:

$$\phi(\alpha,\beta) = B(f_\beta - \sigma_0)/(f_\alpha - \sigma_0) \tag{59}$$

We propose five different series of several tests each divided into two groups. In the first group consisting of series A, B, and C, we will first increase σ_θ to a small positive value and hold it approximately constant. Then, for all further motion S will move in a plane cross section of Fig. 2 as shown in Fig. 3a. In the second group, series D and E, we hold $\tau_{\theta z} = 0$ so that all motion of S takes place in the cross section shown in Fig. 3b.

Test Series A. In the first two phases we hold $\tau_{\theta z} = 0$ and increase $\sigma_z = \sigma$ to a value of σ_1. During phase 2, S will be on face Z_{BC}, hence in Eq. (59) $f_\alpha = \sigma$, and we may write the final value of (59) as

$$\phi(Z_{BC},\beta) = B(f_\beta-\sigma_0)/(\sigma_1-\sigma_0) \qquad (60)$$

During loading, it follows from Eqs. (55) and (58) that

$$\dot\varepsilon_\theta = -\nu\dot\sigma/E \qquad (61a)$$

$$\dot\varepsilon_z = \dot\sigma/E \qquad \sigma < \sigma_0 \qquad (61b)$$

$$\dot\varepsilon_z = \dot\sigma(1/E+1/B) \qquad \sigma > \sigma_0 \qquad (61c)$$

The best-fitting bilinear curve to this data will provide values of E, B, and σ_o for the given material in accord with (61 b,c) and (61a) will then give a value for ν.

We now consider the specific tests. In test A1 we unload σ to zero and increase $\tau_{\theta z} = \tau$ until we detect yield. From Fig. 3a we see that the yielding will be on face X hence $f_\beta = 2\tau$, and from Table 3, $\phi(Z_{BC},X) = G$. Therefore Eq.(61) shows that

$$G = B\frac{2\tau-\sigma_0}{\sigma_1-\sigma_0} \qquad (62a)$$

which determines the constant G.

In test A2 we decrease σ through zero to reverse yield on face Z_{FA}. Now $f_\beta = \sigma_\theta - \sigma_z - \sigma_0$ and $\phi = J$, hence J is given by

$$J = B\,\frac{\sigma_\theta-\sigma_z-\sigma_0}{\sigma_1-\sigma_0} \qquad (62b)$$

In test A3 we decrease σ to $3\sigma_0/4$ and then increase $\tau_{\theta z} = \tau$ to yield on face Y_{BC}. The proper change of subscripts in Eq. (7) shows that $f_\beta = (6\sigma_z + 8\tau)/7$ and from Table 2 $\phi(Z_{BC}, Y_{BC}) = (6B + C)/7$. Substitution into (61) and solution for C furnishes

$$C = B\,\frac{8\tau-6\sigma_1+7\sigma_0/2}{\sigma_1-\sigma_0} \qquad (62c)$$

Finally, in test A4 we decrease σ to $-3\sigma_0/4$ and then increase $\tau_{\theta z} = \tau$ to yield on face Y_{FA}. The resulting formula can be written

$$C = B\,\frac{6\sigma_0+8\tau-5\sigma_0/2}{\sigma_1-\sigma_0} - 6J \qquad (62d)$$

Assuming J is known, comparison of the values of C in (62c,d) gives some measure of the validity of the theory.

Test series B. As in series A, σ_θ has a small positive constant value, but we now hold $\sigma_z = 0$ in phases 1 and 2 and increase τ to a value τ_1 at the end of stage 2. Since this loading is plastic on face X, Eq. (59) assumes the form

$$\phi(X,\beta) = B\,\frac{f_\beta-\sigma_0}{2\tau_1-\sigma_0} \qquad (63)$$

In test B1 we decrease τ through zero to yield on face X', whence Eq. (63) provides a formula for I:

$$I = B\,\frac{-2\tau-\sigma_0}{2\tau_1-\sigma_0} \qquad (64a)$$

In test B2 we decrease τ to zero and then increase $\sigma_z = \sigma$ to yield on face Z_{BC} which results in the formula

$$G = B\,\frac{\sigma-\sigma_0}{2\tau_1-\sigma_0} \qquad (64b)$$

Again, the agreement between (64b) and (62a) tests the validity of the model.

In tests B3 and B4 we reduce τ to $\pm 5\sigma_0/16$, then increase $\sigma_z = \sigma$ to yield on faces Y_{BC} or Y'_{BC} and provide us with formulas for D and H, respectively:

$$D = \frac{B}{3}\,\frac{6\sigma-8\tau_1-\sigma_0/2}{2\tau_1-\sigma_0} \qquad (64c)$$

$$H = \frac{B}{7}\,\frac{6\sigma-9\sigma_0/2}{2\tau_1-\sigma_0} \qquad (64d)$$

Test series C. We again start with a small positive constant σ_θ but in this series we load by increasing σ_z to

$3\sigma_0/4$, then increasing $\tau_{\theta z} = \tau$ to a value τ_1 somewhat beyond yield on face Y_{BC}. We unload both σ_z and τ to zero. In test C1 we then increase τ to yield on face X to obtain an alternative formula for D:

$$D = \frac{B}{3}\,\frac{98\tau-32\tau_1-39\sigma_0}{8\tau_1-5\sigma_0/2} \tag{65a}$$

In test C2 we decrease τ to yield on face X' to obtain an alternative formula for H:

$$H = B\,\frac{7(-2\tau-\sigma_0)}{8\tau_1 - 5\sigma_0/2} \tag{65b}$$

Finally, in test C3 we first decrease σ_z to $-3\sigma_0/4$, and then decrease τ to yield on face Y'_{FA}. The result is an alternative formula for I:

$$I = \frac{49B}{13}\,\frac{6\sigma_\theta-8\tau-5\sigma_0/2}{8\tau_1-5\sigma_0/2} - \frac{36J}{13} \tag{65c}$$

Test series D. We first increase the pressure p to a value p_1 somewhat greater than $\sigma_0 h/a$ thus producing yielding on face Z_{AB}, then unload to $p = \sigma_0 h/2a$. In tests D1 and D2, respectively, we than increase or decrease F to produce yielding on faces Z_{BC} or Z_{FA} with the resulting formulas for A:

$$A = B\,\frac{\pm F/2\pi ah - \sigma_0/4}{p_1 a/h - \sigma_0} \tag{66a,b}$$

Test series E. We increase p only to the value $\sigma_0 h/2a$ in the elastic range, then increase F somewhat past yield on fact Z_{BC} to a value F_1. We then decrease F through zero until yield on face Z_{FA}. The result will be an

alternative formula for J:

$$J = B\,\frac{-F/2\pi ah - 3\sigma_0/4}{F_1/2\pi ah - 3\sigma_0/4} \tag{67}$$

In summary, we have outlined 14 tests to be carried out on closed thin-walled tubes. Each test provides values for E, σ_0, and B in phases 1 and 2; most of them also furnish ν. Each of the other constants is determined by phase 4 of two different tests as listed in Table 5. The tests are independent except that J must be determined from test A2 for E before tests A4 or C3 may be used for a second evaluation of C or I, respectively.

8. Conclusions. We have presented a piecewise linear theory for an initially isotropic strain-hardening elastic-plastic material in a state of plane stress under the following assumptions.

1. The initial yield condition is the 20-faced polyhedron defined in Fig. 2 and Table 1.
2. The material follows Hooke's law for an isotropic material elastically and follows the plastic potential law with a single hardening constant B for any of the 20 faces of the yield polyhedron.
3. For each edge and corner there is a unique linear relation between the stress rates and plastic strain rates, which does not violate the plastic potential law, which is defined symmetrically on symmetric edges or corners, and such that the laws for faces, edges, and corners are internally consistent.
4. During hardening each face moves only in translation and the motion is such that faces, edges, and corners

are neither created for destroyed.

5. When the stress point S is on a given face α the motion $\dot{f}_\alpha$ of that face is such that S stays on α, and the motion of any other face β is given by

$$\dot{f}_\beta = (1/B)\phi(\alpha,\beta)\dot{f}_\alpha \qquad (68)$$

where $\phi(\alpha,\beta) = \phi(\beta,\alpha)$, faces β which are symmetrically located with respect to α will have the same ϕ, and ϕ is the same for all opposite pairs of faces.

We have shown that the most general material which satisfies all of the above assumptions is defined by 11 material constants and have proposed a set of 14 simple experiments to determine each constant at least twice. Obviously the degree of agreement between the different tests for each constant will be a valuable ingredient in deciding upon the adequacy of the model.

There is obviously nothing sacred about the particular 20-faced polyhedron chosen for the initial yield condition. The analysis of a different 20-faced figure defined by different values in Table 1 could be carried out in exactly the same way. Also, polyhedrons with more or fewer faces could be considered. However, a word of caution is in order here. An attempt was made to develop a theory for an 18-faced polyhedron in which the faces X and X' were each collapsed to a point. However, when we came to consider allowable face motions during hardening, the requirement that all six faces Y intersect at a single point was so severe that no hardening other than isotropic was allowed. This is not surprising when we consider that the requirement that only four sides intersect at the point B_2 as discussed in Sec. 4 reduces the total number of hardening

constants from 15 to 8. Pursuing this line of reasoning, we see that if all faces of the polyhedron were triangular we have a much larger number of material constants to determine and hence much more flexibility in fitting the theory to a real material.

A similar approach can be used for a material which is not initially isotropic. The number of degrees of freedom allowed would be so great as to render a general phenomenological discussion meaningless, but experiments could be devised to determine constants for any particular anisotropic material.

The stress-strain curve of a real material is not, of course bilinear, and it may be desirable to use 2 or more plastic hardening constants B', B", etc. in different ranges. Similarly, it may be desirable to replace (6b) by a multi-linear expression. These extensions can be carried out quite easily by using the concept of a "mechanical sub-layer" model [7-9].

This concept is particularly simple for plane stress problems which are solved by finite-element methods, since in this case the model can be thought of as a physical one. Each node is thought of as a pin of finite length which goes through two or more planes of elements which are geometrically identical but have different material properties. By using a sufficient number of layers almost any non-linear relations of hardening or motion can be approximated with any desired degree of accuracy.

REFERENCES

1. Philip G. Hodge, Jr. and Irwin Berman: Piecewise linear strainhardening Plasticity, "Constitutive Equations in Viscoplasticity", J.A. Stricklin and K.J. Saczalski, eds., AMD Vol. 20, ASME, New York, 1976.

2. I. Berman and P.G. Hodge, Jr.: A general theory of piecewise linear plasticity for initially anisotropic materials, Nadbithaka Z Archiwum Mechaniki Stosowanej, 11, 514-540 (1959).

3. P.G. Hodge, Jr.: A general theory of piecewise linear plasticity based on maximum shear, J. Mech. Phys. Solids 5, 242-260 (1957).

4. R.v. Mises: Mechanik der festen Koerper im plastisch deformablem Zustand, Goettinger Nachr. math.-phys. Kl 1913, 582-592 (1913).

5. H. Tresca: Mémoire sur l'écoulement des corps solides, Mém. pres. par div. sav., 18, 733-799 (1868).

6. R.v. Mises: Mechanik der plastischen Formaenderung von Kristallen, Z. angew. Math. Mech., 8, 161-185 (1928).

7. D.K. Vaughan: A comparison of current work-hardening models used in the analysis of plastic deformations, Ms. Thesis, Texas A & M Univ., 1973.

8. G.N. White, Jr.: Application of the theory of perfectly plastic solids to stress analysis of strain hardening solids, GDAM Rep. 51, Brown University, 1950.

9. J.F. Besseling: A theory of plastic flow for anisotropic hardening of an initially isotropic material, Re. S410, Nat. Aero. Res. Inst., Amsterdam, 1953.

Vertex	$\sigma_x(\sigma_\theta)$ $(\sigma_{11}-\sigma_{33})$	$\sigma_y(\sigma_z)$ $(\sigma_{22}-\sigma_{33})$	$\sigma_{11}-\sigma_{22}$
A_i	σ	0	σ
B_i	σ	σ	0
C_i	0	σ	$-\sigma$
D_i	$-\sigma$	0	$-\sigma$
E_i	$-\sigma$	$-\sigma$	0
F_i	0	$-\sigma$	σ

(a)

Plane (i)	σ/σ_0	τ_{xy}/σ_0 (τ_{12}/σ_0)
1	1/2	1/2
2	1	1/8
2'	1	-1/8
1'	1/2	-1/2

(b)

Table 1. Initial Yield Condition

Face X	$B\dot{\varepsilon} = 4\dot{\tau}(0,0,0,1)$
Face Y_{AB}	$B\dot{\varepsilon} = (4/49)[3(\dot{\sigma}_1-\dot{\sigma}_3)+4\dot{\tau}](3,0,-3,4)$
Face Z_{AB}	$B\dot{\varepsilon} = (\dot{\sigma}_1-\dot{\sigma}_3)(1,0,-1,0)$
Edge B_2B_2'	$\dot{\sigma}_i-\dot{\sigma}_3 = B\dot{\varepsilon}_i + A\dot{\varepsilon}_j \qquad \dot{\gamma} = 0$
Edge B_1B_2	$3(\dot{\sigma}_i-\dot{\sigma}_3)+4\dot{\tau} = (1/12)[49B\dot{\varepsilon}_i+(13B+36A)\dot{\varepsilon}_j]$ $\dot{\gamma} = (4/3)(\dot{\varepsilon}_1+\dot{\varepsilon}_2)$
Edge A_2B_2	$\dot{\sigma}_1-\dot{\sigma}_3 = B\dot{\varepsilon}_1 + C\dot{\gamma}/8 \qquad \dot{\varepsilon}_2 = 0$ $\dot{\tau} = C\dot{\varepsilon}_1/8 + (13B - 12C)\dot{\gamma}/64$
Edge A_1B_1	$\dot{\sigma}_1-\dot{\sigma}_3 = (11B-8D)\dot{\varepsilon}_1/12 + D\dot{\gamma}/4$ $\dot{\tau} = (D\dot{\varepsilon}_1 + B\dot{\gamma})/4 \qquad \dot{\varepsilon}_2 = 0$
Corner B_2	$\dot{\sigma}_i-\dot{\sigma}_3 = B\dot{\varepsilon}_i + A\dot{\varepsilon}_j + C\dot{\gamma}/8$ $\dot{\tau} = C(\dot{\varepsilon}_1+\dot{\varepsilon}_2)/8 + (13B-12C)\dot{\gamma}/64$
Corner B_1	$\dot{\sigma}_i-\dot{\sigma}_3 = (11B-8D)\dot{\varepsilon}_i/12+ (12A-B-8D)\dot{\varepsilon}_j/12 + D\dot{\gamma}/4$ $\dot{\tau} = (1/4)[D(\dot{\varepsilon}_1+\dot{\varepsilon}_2) + B\dot{\gamma}]$

Table 2 Summary of Flow Laws

Note: i,j = 1,2 with $i \neq j$

β/α	X	Y_i	Z_i	Y_i'	X'
X	B	(3D+4B)/7	G	H	I
Y_i	(3D+4B)/7	(36λ+13B)/49	(6λ+C)/7	(36λ+13I)/49	H
Z_i	G	(6λ+C)/7	λ	(6λ+C)/7	G
Y_i'	H	(36λ+13I)/49	(6λ+C)/7	(36λ+13B)/49	(3D+4B)/7
X'	I	H	G	(3D+4B)/7	B

(a) $\phi(\alpha,\beta)$

i/j	AB	BC	CD	DE	EF	FA
AB	B	A	J	I	J	A
BC	A	B	A	J	I	J
CD	J	A	B	A	J	I
DE	I	J	A	B	A	J
EF	J	I	J	A	B	A
FA	A	J	I	J	A	B

(b) λ

Table 3 Definition of $\phi(\alpha,\beta)$

Face-Edge-Face	Inequalities
$Y_{AB}-A_1B_1-X$	$\frac{3D+4B}{11B-4D} \leq \frac{\dot{\tau}}{\dot{\sigma}_1-\dot{\sigma}_3} \leq \frac{B}{D}$
$Z_{AB}-A_2B_2-Y_{AB}$	$\frac{C}{B} \leq \frac{8\dot{\tau}}{\dot{\sigma}_1-\dot{\sigma}_3} \leq \frac{13B-6C}{6B+C}$
$Y_{BC}-B_1B_2-Y_{AB}$	$\frac{13B+36A}{49B} \leq \frac{3(\dot{\sigma}_1-\dot{\sigma}_3)+4\dot{\tau}}{3(\dot{\sigma}_2-\dot{\sigma}_3)+4\dot{\tau}} \leq \frac{49B}{13B+36A}$
$Z_{BC}-B_2B'_2-Z_{AB}$	$\frac{A}{B} \leq \frac{\dot{\sigma}_1-\dot{\sigma}_3}{\dot{\sigma}_2-\dot{\sigma}_3} \leq \frac{B}{A}$

Table 4a Edge inequalities

Edge-Corner-Edge	Inequalities
$C_1B_1-B_1-B_1A_1$	$\frac{3D\dot{\tau}-12B(\dot{\sigma}_2-\dot{\sigma}_3)}{11B+3D} \leq \frac{B-D}{B-A}(\dot{\sigma}_1-\dot{\sigma}_2) \leq \frac{12B(\dot{\sigma}_1-\dot{\sigma}_3)-3D\dot{\tau}}{11B+3D}$
$B_2B_1-B_1-\ldots$	$(3D+4B)(\dot{\sigma}_1+\dot{\sigma}_2-2\dot{\sigma}_3) \leq (12A+10B-8D)\dot{\tau}$
$B'_1B_2-B_2-B_2B_1$	$\frac{2C}{A+B} \leq \frac{16\dot{\tau}}{\dot{\sigma}_1+\dot{\sigma}_2-2\dot{\sigma}_3} \leq \frac{13B-6C}{3A+3B+C}$
$C_2B_2-B_2-B_2A_2$	$\frac{8C\dot{\tau}-(13B-12C)(\dot{\sigma}_2-\dot{\sigma}_3)}{(13B+C)(B-C)} \leq \frac{\dot{\sigma}_1-\dot{\sigma}_2}{B-A} \leq \frac{(13B-12C)(\dot{\sigma}_1-\dot{\sigma}_3)-8C\dot{\tau}}{(13B+C)(B-C)}$

Table 4b Corner Inequalities

Constant	A	C	D	G	H	I	J
Tests	D1	A3	B3	A1	B4	B1	A2
	D2	A4	C1	B2	C2	C3	E

Table 5 Experiments

Edge or Corner	Artificial stress point motions
A_1B_1	$\dot{t}_X \equiv 2\dot{\tau} = (B/6)(-4\dot{\epsilon}_1 + 3\dot{\gamma})$ $\dot{t}_{YAB} \equiv (2/7)[3(\dot{\sigma}_1-\dot{\sigma}_3)+4\dot{\tau}] = (7B/6)\dot{\epsilon}_1$
A_2B_2	$\dot{t}_{YAB} = (7B/8)\dot{\gamma}$ $\dot{t}_{ZAB} \equiv \dot{\sigma}_1-\dot{\sigma}_3 = (B/4)(4\dot{\epsilon}_i-3\dot{\gamma})$
B_1B_2	$\dot{t}_{YAB} = (7B/6)\dot{\epsilon}_1$ $\dot{t}_{YBC} \equiv (2/7)[3(\dot{\sigma}_2-\dot{\sigma}_3)+4\dot{\tau}] = (7B/6)\dot{\epsilon}_2$
B_2B_2'	$\dot{t}_{ZAB} = B\dot{\epsilon}_1$ $\dot{t}_{ZBC} \equiv \dot{\sigma}_2-\dot{\sigma}_3 = B\dot{\epsilon}_2$
B_1	$\dot{t}_X = (B/6)[-4(\dot{\epsilon}_1+\dot{\epsilon}_2)+3\dot{\gamma}]$ $\dot{t}_{YAB} = (7B/6)\dot{\epsilon}_1$ $\dot{t}_{YBC} = (7B/6)\dot{\epsilon}_2$
B_2	$\dot{t}_{YAB} = (7B/72)(3\dot{\epsilon}_1 - 3\dot{\epsilon}_2 + 4\dot{\gamma})$ $\dot{t}_{YBC} = (7B/72)(-3\dot{\epsilon}_1 + 3\dot{\epsilon}_2 + 4\dot{\gamma})$ $\dot{t}_{ZAB} = (B/8)(6\dot{\epsilon}_1 + 2\dot{\epsilon}_2 - 3\dot{\gamma})$ $\dot{t}_{ZBC} = (B/8)(2\dot{\epsilon}_1 + 6\dot{\epsilon}_2 - 3\dot{\gamma})$

Table 6 Motions due to edge and corner stress points

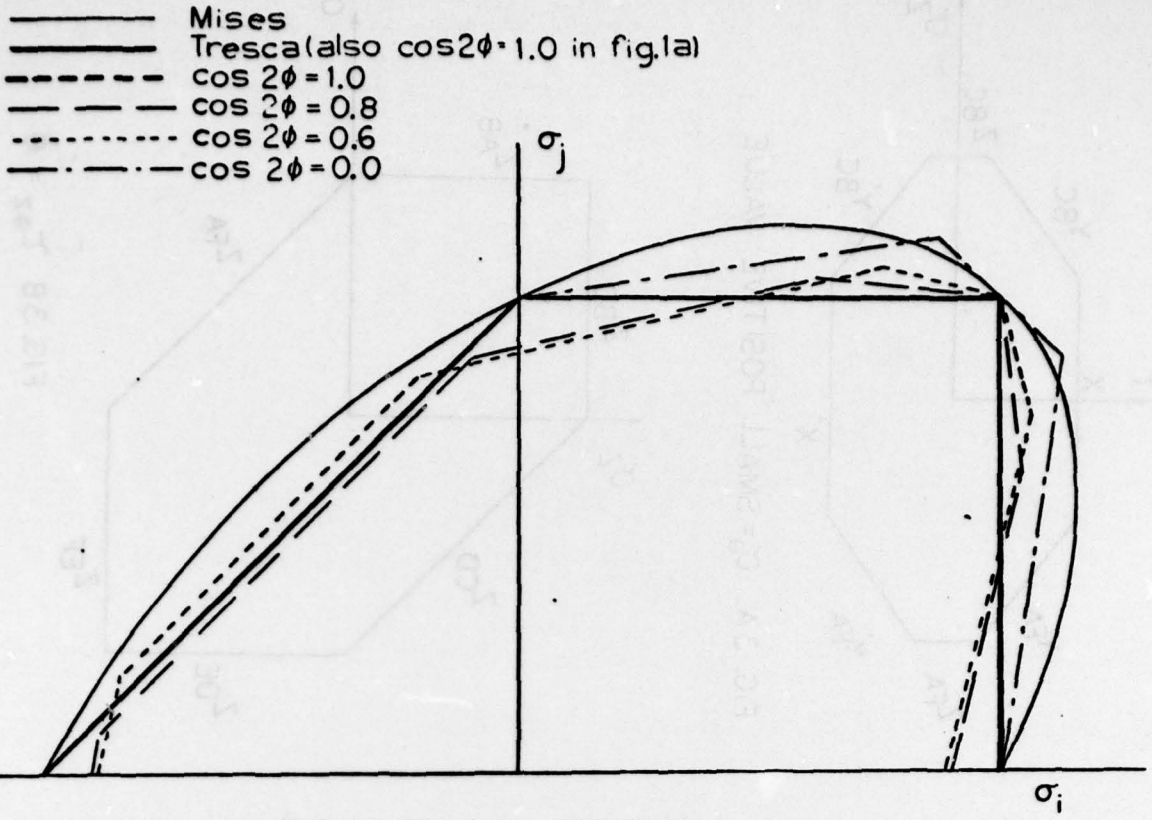

FIG. 1A BIAXIAL TENSION

FIG. 1B TENSION-TORSION

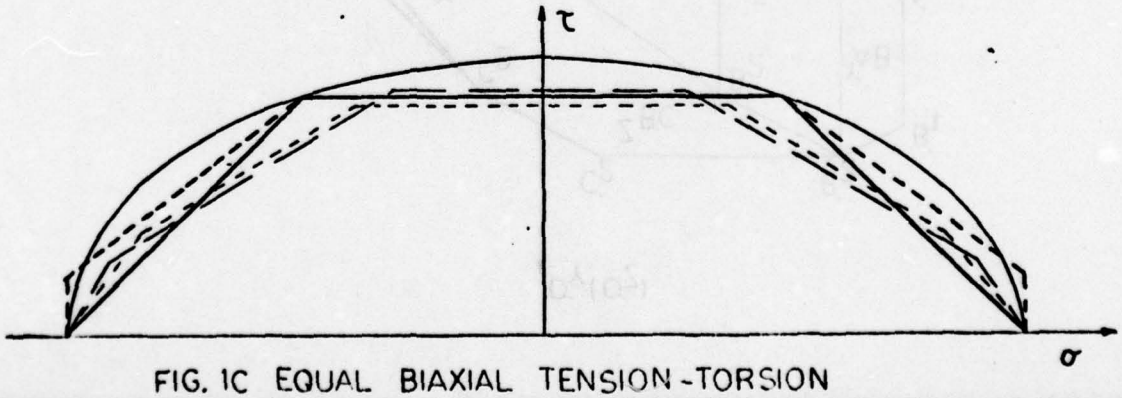

FIG. 1C EQUAL BIAXIAL TENSION-TORSION

FIG. 3A σ_θ = SMALL POSITIVE VALUE

FIG. 3B $\tau_{\theta z} = 0$

FIG. 2
INITIAL YIELD CONDITION

APPENDIX

Motion of sides when stress point is on an edge or corner.

When the stress point S is on edge A_1B_1, the actual motion of the adjacent faces X and Y_{AB} must be such that S remains on both of them. Thus, taking the motion of S from Table 2, we see that

$$\dot{f}_X \equiv 2\dot{\tau} = (D\dot{\epsilon}_1 + B\dot{\gamma})/2 \tag{A1}$$

$$\dot{f}_{YAB} \equiv (2/7)[3(\dot{\sigma}_1-\dot{\sigma}_3)+4\dot{\tau}] = [(11B-4D)\dot{\epsilon}_1 + (3D+4B)\dot{\gamma}]/14$$

Consider now two artificial stress points S_1 and S_2 which are on edge A_1B_1 but where S_1 is associated with face X and S_2 with Y_{AB}. Let S_1 alone move according to

$$\dot{f}'_X \equiv 2\dot{\tau} = B(a\dot{\epsilon}_1 + b\dot{\gamma}) \tag{A2}$$

and S_2 according to

$$\dot{f}''_{YAB} \equiv (2/7)[3(\dot{\sigma}_1-\dot{\sigma}_3) + 4\dot{\tau}] = B(c\dot{\epsilon}_1 + d\dot{\gamma}) \tag{A3}$$

where $\dot{\epsilon}_1$ and $\dot{\gamma}$ are the actual strain rates associated with S. The constants a, b, c, and d are to be determined so that the resultant motion of faces X and Y_{AB} due to both S_1 and S_2 is the same as that due to S. According to Table 2, the motion of Y_{AB} due to S_1 is $(1/7)(3D+4B)\,\dot{f}'_X/B$ where $\dot{f}'_X$ is given by (A2). Therefore the resultant motion of Y_{AB} is

$$\dot{f}_{YAB} = (1/7)(3D+4B)(a\dot{\epsilon}_1+b\dot{\gamma}) + B(c\dot{\epsilon}_1+d\dot{\gamma}) \tag{A4a}$$

Similarly, the resultant motion of X is

$$\dot{f}_X = B(a\dot{\epsilon}_1+b\dot{\gamma}) + (1/7)(3D+4B)(c\dot{\epsilon}_1 +d\dot{\gamma}) \tag{A4b}$$

The expressions for $\dot{f}_X$ and $\dot{f}_{YAB}$ given by (A1) and (A4) are to be

the same for all motions of S, i.e., for all choices of $\dot{\epsilon}_1$ and $\dot{\gamma}$. This requirement leads to four linear equations for a, b, c, and d whose solution is

$$a = -2/3 \quad b = 1/2 \quad c = 7/6 \quad d = 0 \tag{A5}$$

Therefore, the artificial motions separately are

$$S_1: \quad \dot{f}_X \equiv 2\dot{\tau} = (B/6)(-4\dot{\epsilon}_1 + 3\dot{\gamma}) \tag{A6}$$

$$S_2: \quad \dot{f}_{YAB} \equiv (2/7)[3(\dot{\sigma}_1-\dot{\sigma}_3) + 4\dot{\tau}] = (7B/6)\dot{\epsilon}_1$$

We now state that by definition the motion of any other face of the yield polyhedron due to S is the resultant of that due to S_1 and S_2 as defined by (A6). For example, it follows from Table 2 that the motion of face Y_{BC} is

$$\begin{aligned}\dot{f}_{YBC} &\equiv (2/7)[3(\dot{\sigma}_2-\dot{\sigma}_3) + 4\dot{\tau}] \\ &= (1/7)(3D+4B)(-4\dot{\epsilon}_1+3\dot{\gamma})/6+(1/49)(36A+13B)\dot{\epsilon}_1/6 \\ &= (1/14)[(12A-B-4D)\dot{\epsilon}_1+(4B+3D)\dot{\gamma}]\end{aligned} \tag{A7}$$

A similar computation will yield the motion of any other side due to the motion of a stress point on A_1B_1.

Therefore, we see that the only thing necessary to define all motions for stress points on edges is to determine the equivalent motions of artificial stress points on the adjoining sides. This is easily done by the same method as above for edge A_1B_1; the results are summarized in Table 6.

If the stress point is in corner B_1, a similar approach must be used except that there will now be three artificial stress points and S will have three degrees of freedom. The

actual motion of the three faces due to S is

$$\dot{f}_X = (1/2)[D(\dot{\epsilon}_1+\dot{\epsilon}_2)+B\dot{\gamma}]$$

$$\dot{f}_{YAB}=(1/14)[(11B-4D)(\dot{\epsilon}_1+\dot{\epsilon}_2)+12(A-B)\dot{\epsilon}_2+(3D+4B)\dot{\gamma}] \qquad (A8)$$

$$\dot{f}_{YBC} = (1/14)[(11B-4D)(\dot{\epsilon}_1+\dot{\epsilon}_2)+12(A-B)\dot{\epsilon}_1+(3D+4B)\dot{\gamma}]$$

and the general forms for the motions of artificial stress points are

$$S_1: \quad \dot{f}'_X = B[a(\dot{\epsilon}_1+\dot{\epsilon}_2)+b\dot{\gamma}]$$

$$S_2: \quad \dot{f}''_{YAB} = B[c(\dot{\epsilon}_1+\dot{\epsilon}_2)+d\dot{\epsilon}_2+e\dot{\gamma}] \qquad (A9)$$

$$S_3: \quad \dot{f}''_{YBC} = B[c(\dot{\epsilon}_1+\dot{\epsilon}_2)+d\dot{\epsilon}_1+e\dot{\gamma}]$$

We compute the total motion of each of the three faces due to the combined effect of the three S_i, and demand that it be the same for all choices of $\dot{\epsilon}_1$, $\dot{\epsilon}_2$, and $\dot{\gamma}$. Only five of the resulting nine equations are independent and these are easily solved to give

$$a = -2/3 \quad b = 1/2 \quad c = 7/6 \quad d = -7/6$$
$$e = 0 \qquad (A10)$$

Substitution of (A10) in (A9) gives the specific artificial motions as listed in Table 6.

Corner B_2 is the intersection of four sides whose motions due to S in B_2 are

$$\dot{f}_{YAB} = (1/56)[8(6B+C)(\dot{\epsilon}_1+\dot{\epsilon}_2)+48(A-B)\dot{\epsilon}_2 + (13B-6C)\dot{\gamma}] \qquad (A11)$$

$$\dot{f}_{ZAB} = B(\dot{\epsilon}_1+\dot{\epsilon}_2) + (A-B)\dot{\epsilon}_2 + (C/8)\dot{\gamma}$$

with expressions for $\dot{f}_{YBC}$ and $\dot{f}_{ZBC}$ obtained by interchanging $\dot{\epsilon}_1$ and $\dot{\epsilon}_2$. The motions of the artificial stress points are

$$S_1: \quad \dot{f}'_{YAB} = B[a(\dot{\epsilon}_1+\dot{\epsilon}_2)+b\dot{\epsilon}_2+c\dot{\gamma}]$$
$$S_3: \quad \dot{f}''_{ZAB} = B[d(\dot{\epsilon}_1+\dot{\epsilon}_2)+e\dot{\epsilon}_2+f\dot{\gamma}] \qquad (A12)$$

with S_2 and S_4 obtained by interchanging $\dot{\epsilon}_1$ and $\dot{\epsilon}_2$ above.

Comparing the total resultant motions with the actual ones we obtain 12 equations of which only 5 are independent. The most general solution may be written

$$a = (7/24)(1-\mu) \quad b = (7/12)(\mu-1) \quad c = 7/16$$
$$d = (3+\mu)/4 \quad e = -(1+\mu)/2 \quad f = -3/8 \qquad (A13)$$

for any value of μ. However, μ has no physical meaning so that without loss of generality we may set it equal to zero, thus leading to the final lines in Table 6.